Performance Limits of Spatially Distributed Molecular Communications With Receiver Saturation

Flavio Zabini, *Member, IEEE*, and Barbara Maví Masini, *Senior Member, IEEE*

***Abstract*—Molecular communications via diffusion are affected by unreliability and inter symbol interference in case of single transmitter. A promising solution to these issues appears to be the adoption of a swarm of randomly distributed transmitting nano-devices and a single spherical receiver. However, such a perspective assumes the receiver as fully absorbing (i.e., able to absorb an unlimited number of molecules per second). In this letter, we show that, if this assumption is relaxed, increasing the number of point transmitters leads to a saturation effect which makes communication impossible when digital transmission is considered. By means of a first and second order spatio-temporal stochastic model, we analytically derive the maximum allowed point transmitters density before saturation arises, as a function of parameters such as the diffusion coefficient, the maximum number of absorbed molecules, and the number of previously transmitted symbols. The analysis is validated via Monte Carlo simulation.**

***Index Terms*—Molecular communications, diffusion, point processes, asynchronous transmission, spatiotemporal model.**

I. Introduction

MOLECULAR communications have recently attracted an increasing interest for providing many bio-inspired communication methods for both nanoscale (e.g., nanorobots for surgical instrumentation, diagnosis, and drug delivery) and macroscale (e.g., underwater communication) applications [1]. In molecular communication via diffusion (MCvD), the Brownian motion of chemical molecules substitutes electromagnetic waves as information carrier [2], [3], [4]. Crucial aspects such as noise, interference, and capacity have been investigated in the literature [5], [6], [7], [8]: as a matter of fact, bionanomachines for molecular communications are small in scale, limited and unreliable in functionality. Hence, it is their collective behavior that has to be studied, instead of considering them individually.

In this context, the authors in [9] proposed a model with a swarm of point transmitters spatially distributed according to a homogeneous Poisson point process (HPPP), and a spherical receiver. The collective strength of such a communication system is evaluated both in terms of received number of molecules and of bit error probability (BEP) when on-off keying (OOK) digital modulations is considered. These results have been extended in case of asynchronous transmissions, i.e., without assuming that all point transmitters emit molecules at the same time instants, in [10], [11], [12].

Two of the most relevant results regarding this kind of spatially distributed MCvD scenario can be summarized as follows: i) from a single transmitter MCvD scenario, the signal-to-noise ratio (SNR) saturates (i.e., when digital transmission is considered, the BEP shows a floor) as the number of emitted molecules increases; ii) both SNR and the signal-to-noise-plus-interference ratio (SNIR) linearly increase (thus, the BEP decreases) as the spatial density of point transmitter increases. In other words, indefinitely increasing the density of point transmitters (rather than increasing the number of transmitted molecules for each point transmitter) appears as the key-solution to counteract both noise and inter-symbol interference (ISI) effects. However, this result clearly depends on the ideal assumption that the receiver can indefinitely absorb all molecules hitting its surface (i.e., fully absorbing receiver). But, in [13], it is shown that the absorbing rate is limited for chemical reasons and, in [14], the number of molecules absorbed within a certain interval (i.e., a bit interval) is thus considered bounded by a certain threshold. The problem of the receiver congestion when the fully absorbing assumption is removed has also been addressed in [15], where an algorithm is proposed to control molecules emission and avoid molecules wasting. However, [13], [14], [15] deal with a point-to-point molecular communication scenario.

Differently, in this work, we address a scenario with a swarm of point transmitters to study the effect of the receiver saturation in the terms of BEP. In addition, differently from [15], which is focused on an early congestion detection and a proper run-time molecules emission control in a point-to-point communication scenario, we analytically derive the maximum value of the point transmitters density before the congestion arises for a fixed emission rate.

II. System Model

We consider a large-scale molecular communications scenario similar to that presented in [9] with a swarm of point transmitters and a spherical receiver (see Fig. 1). More specifically, the transmitters positions $\{\mathbf{x}_k\}$ are a random set given by the outcomes of a spatial HPPP Π with intensity λ_{a} restricted to $\Omega_{R_{\mathrm{a}}} \setminus \Omega_R$, where $\Omega_{R_{\mathrm{a}}}$ and Ω_R are spheres of radius R_{a} and R, respectively.

Manuscript received 21 February 2022; revised 28 July 2022 and 9 November 2022; accepted 23 November 2022. Date of publication 1 December 2022; date of current version 22 March 2023. The associate editor coordinating the review of this article and approving it for publication was H. B. Yilmaz. *(Corresponding author: Flavio Zabini.)*

Flavio Zabini is with the DEI and CNIT/WiLab, University of Bologna, 40136 Bologna, Italy (e-mail: flavio.zabini2@unibo.it).

Barbara Maví Masini is with the Institute of Electronics, Information Engineering and Telecommunications, National Research Council, 40136 Bologna, Italy, and also with CNIT/WiLab, 40136 Bologna, Italy (e-mail: barbara.masini@cnr.it).

Digital Object Identifier 10.1109/TMBMC.2022.3225740

This work is licensed under a Creative Commons Attribution 4.0 License. For more information, see https://creativecommons.org/licenses/by/4.0/

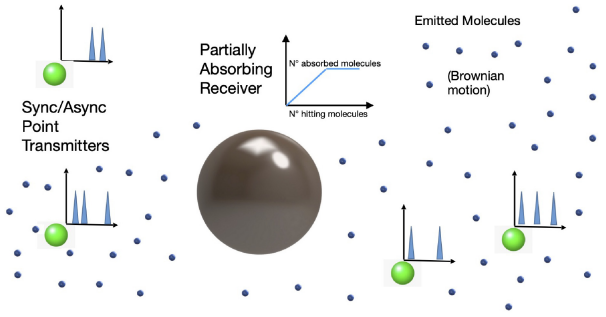

Fig. 1. A swarm of randomly placed point transmitters randomly emit molecules according to independent time-domain PPs with the same intensity function $\varrho(t)$.

For the transmission process, we consider the asynchronous stochastic model proposed in [10], [11], [12]. The instants in which the molecules are emitted by the k-th point transmitter are given by the random set $\{\boldsymbol{\tau}_l^{(k)}\}$ constituted by the output of the (generally, non stationary) time domain PP $\Phi^{(k)}$ (i.e., $\boldsymbol{\tau}_l^{(k)}$ is the emission instant of the l-th molecule emitted by the k-th transmitter placed at $\mathbf{x}_k$). The time domain PPs $\{\Phi^{(k)}\}$ are independent and have the same intensity function $\rho(t)$. Such an asynchronous model describes a scenario where the point transmitters represents the randomly located points where spontaneous emissions happen in the fluid due to chemical reactions. Since the emissions are related to the collisions between the reagent molecules, it must be highlighted that the Brownian motion of the reagent molecules motivates the independence among the time domain PPs and $\rho(t)$ takes the meaning of the propensity function as described by [16].

Note that, the aforementioned asynchronous transmissions (also known as timing transmissions) can be reduced to the synchronous case (also known as Poisson concentration transmission) by setting $\rho(t) = N_{\mathrm{tx}}\delta(t)$, where N_{tx} is the average number of molecules instantaneously emitted by a Poisson concentration transmitter and $\delta(t)$ is the Dirac delta. In such a case, the model reduces to the synchronous scenario proposed in [9], where the point transmitters represent nano-machines which collaborate to transmit the messages.

The key difference with respect to the spatiotemporal model in [10] and [12] is at the receiver side. Here, the goal is to investigate the impact of the saturation effect on a spatially distributed molecular communication system. Thus, instead of assuming a fully absorbing receiver, we take into account the effect of saturation by means of the maximum absorbing rate f_{sat}, indicating the number of molecules per second that the receiver can absorb. For the sake of simplicity, we assume that the maximum number of absorbed molecules for each symbol time results in $\overline{N}_{\mathrm{abs}} = f_{\mathrm{sat}}\, T_{\mathrm{b}}$ and that such a level is quickly resetted at each timestep. This is in accordance with the model proposed in [14] (establishing a more complex and accurate model for the reception mechanism, e.g., based on ligand-receptor interactions, is beyond the scope of the present letter). Thus, the random variable (RV) $\mathsf{n}_{\mathrm{abs}}$ denoting the total number of absorbed molecules is given by

$$\mathsf{n}_{\mathrm{abs}} = \min\left\{\overline{N}_{\mathrm{abs}}, \mathsf{n}_{\mathrm{rx}}\right\} \tag{1}$$

where n_{rx} is the number of absorbed molecules (within T_{b}) when a fully absorbing spherical receiver of radius R is considered with hitting rate [3]

$$f_{\mathrm{hit}}(d,t) = \frac{R}{d}\frac{1}{\sqrt{4\pi D t}}\frac{d-R}{t}\exp\left[-\frac{(d-R)^2}{4Dt}\right] \tag{2}$$

being d the distance from the transmitter, D the diffusion coefficient, and t the time after the transmission of the unitary molecule. As known, $f_{\mathrm{hit}}(d,t)$ represents the (infinitesimal) probability that a molecule emitted at the time origin at distance d is received (exactly) at time t. The probability that a molecule emitted at $t = 0$ is observed within the interval $[t_0, t_0 + T_{\mathrm{b}}]$ is thus given by

$$\int_{t_0}^{t_0+T_{\mathrm{b}}} f_{\mathrm{hit}}(d,t)dt = F_{\mathrm{hit}}(d, t_0 + T_{\mathrm{b}}) - F_{\mathrm{hit}}(d, t_0) \tag{3}$$

where

$$F_{\mathrm{hit}}(d,t) = \frac{R}{d}\,\mathrm{erfc}\left(\frac{d-R}{\sqrt{4Dt}}\right). \tag{4}$$

The time invariance of the Fick's law of diffusion allows to write that, if the emission happens at $\boldsymbol{\tau}_l^{(k)}$, the probability that the molecule is received in the interval $[t_0, t_0 + T_{\mathrm{b}}]$ is

$$F_{\mathrm{hit}}\left(d, t_0 + T_{\mathrm{b}} - \boldsymbol{\tau}_l^{(k)}\right) - F_{\mathrm{hit}}\left(d, t_0 - \boldsymbol{\tau}_l^{(k)}\right) = \overline{F}_{\mathrm{hit}}\left(d, t_0 - \boldsymbol{\tau}_l^{(k)}\right) \tag{5}$$

where $\overline{F}_{\mathrm{hit}}(d,t) \triangleq F_{\mathrm{hit}}(d, T_{\mathrm{b}} + t) - F_{\mathrm{hit}}(d,t)$. Due to the linearity of the Fick's law, the number of received molecules from all transmitters within the interval $[t_0, t_0 + T_{\mathrm{b}}]$ is

$$\mathsf{n}_{\mathrm{rx}}[\rho(t)] = \sum_{\mathbf{x}_k \in \Pi}\sum_{\boldsymbol{\tau}_l^{(k)} \in \Phi^{(k)}} \mathsf{b}_l^{(k)} \tag{6}$$

where the dependence on $\rho(t)$ is highlighted and $\mathsf{b}_l^{(k)}$ is a binomial RV equal to one with probability $\overline{F}_{\mathrm{hit}}(\mathbf{x}_k, t_0 - \boldsymbol{\tau}_l^{(k)})$.

We now consider the digital transmission of $j+1$ symbols, where the intensity function of all transmission processes is modeled by

$$\rho(t) = \sum_{i=0}^{j} \mathsf{a}_i\, g(t - iT_{\mathrm{b}}) \tag{7}$$

where a_i is the i-th bit (which is 1 with probability p_1 and 0 with probability $p_0 = 1 - p_1$), the waveform $g(t)$ is such that $g(t) = N_{\mathrm{tx}}\delta(t)$ for the synchronous Poisson transmission case and $g(t) = (N_{\mathrm{tx}}/T_{\mathrm{a}})\,\mathrm{rect}(t/T_{\mathrm{a}})$ for the asynchronous transmission case, with T_{a} the activity interval and $T_{\mathrm{a}}/T_{\mathrm{b}} \leq 1$ the duty cycle. It has been shown in [10], [11], [12] that $\rho(t)$ plays the role of the input of a linear time invariant (LTI) system, thus the superposition of effects holds. Focusing on the generic j-th instant (due to the causality, the molecules emitted after the j-th bit time provide no effect), the number of hitting molecules can be written as

$$\mathsf{n}_{\mathrm{rx}}|_{\mathsf{a}_{1:j}} = \mathsf{n}_{\mathrm{u}} + \mathsf{n}_{\mathrm{ISI}} \tag{8}$$

where n_{u} is the useful component evaluated by (6) when $\rho(t) = \mathsf{a}_j\, g(t - jT_{\mathrm{b}})$, and $\mathsf{n}_{\mathrm{ISI}}$ is the ISI component evaluated by (6) when $\rho(t) = \sum_{i=1}^{j-1} \mathsf{a}_i\, g(t - iT_{\mathrm{b}})$. Note that the

randomness of the useful component n_{u} represents the noise, while the ISI component $\mathsf{n}_{\mathrm{ISI}}$ is given by the molecules hitting the receiver in a bit interval different than the emission one.

III. Performance Evaluation

A. BEP as a Function of the Threshold

Some analytical expressions derived for the fully absorbing receiver are here properly adapted to calculate the BEP taking the saturation effect into account. From (8), it follows that, if $\mathsf{a}_j = 0$ or $\mathsf{a}_j = 1$, the number n_{rx} of hitting molecules results in $\mathsf{n}_{\mathrm{rx}}|_0 = \mathsf{n}_{\mathrm{ISI}}$ and $\mathsf{n}_{\mathrm{rx}}|_1 = \mathsf{n}_{\mathrm{u}} + \mathsf{n}_{\mathrm{ISI}}$, respectively. According to (1), the number of absorbed molecules in the two cases are thus given by

$$\mathsf{n}_{\mathrm{abs}}|_0 = \min\{\overline{N}_{\mathrm{abs}}, \mathsf{n}_{\mathrm{ISI}}\} \tag{9a}$$

$$\mathsf{n}_{\mathrm{abs}}|_1 = \min\{\overline{N}_{\mathrm{abs}}, \mathsf{n}_{\mathrm{u}} + \mathsf{n}_{\mathrm{ISI}}\}. \tag{9b}$$

The mean and the variance of n_{u} and $\mathsf{n}_{\mathrm{ISI}}$ have been evaluated in [12]. The average BEP can instead be computed as:

$$P_{\mathrm{e}} = p_0 P_{\mathrm{e}}|_0 + p_1 P_{\mathrm{e}}|_1 \tag{10}$$

where, N_{th} denoted the threshold, $P_{\mathrm{e}}|_0 \triangleq \mathrm{Prob}\{\mathsf{n}_{\mathrm{abs}}|_0 > N_{\mathrm{th}}\}$ and $P_{\mathrm{e}}|_1 \triangleq \mathrm{Prob}\{\mathsf{n}_{\mathrm{abs}}|_1 < N_{\mathrm{th}}\}$, where $\mathsf{n}_{\mathrm{abs}}|_0$ and $\mathsf{n}_{\mathrm{abs}}|_1$ represents the number of absorbed molecules conditioned to $\mathsf{a}_j = 0$ and $\mathsf{a}_j = 1$, respectively. By making use of the total probability theorem, we can derive

$$\begin{aligned} P_{\mathrm{e}}|_0 = {} & \mathrm{Prob}\{\mathsf{n}_{\mathrm{abs}}|_0 > N_{\mathrm{th}}, \mathsf{n}_{\mathrm{ISI}} \le \overline{N}_{\mathrm{abs}}\} \\ & + \mathrm{Prob}\{\mathsf{n}_{\mathrm{abs}}|_0 > N_{\mathrm{th}}, \mathsf{n}_{\mathrm{ISI}} > \overline{N}_{\mathrm{abs}}\} \end{aligned} \tag{11a}$$

$$\begin{aligned} P_{\mathrm{e}}|_1 = {} & \mathrm{Prob}\{\mathsf{n}_{\mathrm{abs}}|_1 < N_{\mathrm{th}}, \mathsf{n}_{\mathrm{u}} + \mathsf{n}_{\mathrm{ISI}} \le \overline{N}_{\mathrm{abs}}\} \\ & + \mathrm{Prob}\{\mathsf{n}_{\mathrm{abs}}|_1 < N_{\mathrm{th}}, \mathsf{n}_{\mathrm{u}} + \mathsf{n}_{\mathrm{ISI}} > \overline{N}_{\mathrm{abs}}\}. \end{aligned} \tag{11b}$$

From (9) and (11) one can readily note that the case $N_{\mathrm{th}} > \overline{N}_{\mathrm{abs}}$ makes the error event conditioned to $\mathsf{a}_j = 0$ an impossible event and the error event conditioned to $\mathsf{a}_j = 1$ a certain event. Moroever, the case $N_{\mathrm{th}} < \overline{N}_{\mathrm{abs}}$ can be easily computed by making use of (9). Thus, (11) becomes

$$P_{\mathrm{e}}|_0 = \begin{cases} \mathrm{Prob}\{\mathsf{n}_{\mathrm{ISI}} > N_{\mathrm{th}}\} & \text{for } N_{\mathrm{th}} \le \overline{N}_{\mathrm{abs}} \\ 0 & \text{for } N_{\mathrm{th}} > \overline{N}_{\mathrm{abs}} \end{cases} \tag{12a}$$

$$P_{\mathrm{e}}|_1 = \begin{cases} \mathrm{Prob}\{\mathsf{n}_{\mathrm{u}} + \mathsf{n}_{\mathrm{ISI}} < N_{\mathrm{th}}\} & \text{for } N_{\mathrm{th}} \le \overline{N}_{\mathrm{abs}} \\ 1 & \text{for } N_{\mathrm{th}} > \overline{N}_{\mathrm{abs}} \end{cases} \tag{12b}$$

Denote as μ_{u} and σ_{u}^2 the mean and variance of the useful component n_{u}. Clearly, the ISI component depends on the previously emitted symbols. However, if they are assumed independent and equiprobable, ISI mean μ_{ISI} and variance σ_{ISI}^2 can be calculated obtaining expressions independent on the particular symbols sequences [12]. In [17] it is proved that $\mathsf{n}_{\mathrm{ISI}}$ and $\mathsf{n}_{\mathrm{u}} + \mathsf{n}_{\mathrm{ISI}}$ can be approximated as generalized Gaussian random variables with mean μ_{ISI} and $\mu_{\mathrm{u}} + \mu_{\mathrm{ISI}}$ and variance σ_{ISI}^2 and $\sigma_{\mathrm{u}}^2 + \sigma_{\mathrm{ISI}}^2$, respectively. We recall that the generalized Gaussian probability density function (PDF) is defined as $p(x) = \frac{\beta}{2\alpha\Gamma(1/\beta)} \exp\left[-\left(\frac{x-\mu}{\alpha}\right)^{\beta}\right]$, where $\Gamma(\cdot)$ is the gamma function, μ is the mean, β is the shaping parameter (note that for $\beta = 2$ we obtain the normal distribution), and α is a scale parameter such that the variance results in $\alpha^2 \frac{\Gamma(3/\beta)}{\Gamma(1/\beta)}$. Thus, (12) becomes

$$P_{\mathrm{e}}|_0 = \begin{cases} \frac{1}{2} - \frac{\gamma\left(\frac{1}{\beta}, \left|\frac{N_{\mathrm{th}} - \mu_{\mathrm{ISI}}}{\alpha_0}\right|^{\beta}\right)}{2\,\mathrm{sgn}(N_{\mathrm{th}} - \mu_{\mathrm{ISI}})\Gamma\left(\frac{1}{\beta}\right)} & \text{for } N_{\mathrm{th}} \le \overline{N}_{\mathrm{abs}} \\ 0 & \text{for } N_{\mathrm{th}} > \overline{N}_{\mathrm{abs}} \end{cases} \tag{13a}$$

$$P_{\mathrm{e}}|_1 = \begin{cases} \frac{1}{2} + \frac{\gamma\left(\frac{1}{\beta}, \left|\frac{N_{\mathrm{th}} - \mu_{\mathrm{u}} - \mu_{\mathrm{ISI}}}{\alpha_1}\right|^{\beta}\right)}{2\,\mathrm{sgn}(N_{\mathrm{th}} - \mu_{\mathrm{u}} - \mu_{\mathrm{ISI}})\Gamma\left(\frac{1}{\beta}\right)} & \text{for } N_{\mathrm{th}} \le \overline{N}_{\mathrm{abs}} \\ 1 & \text{for } N_{\mathrm{th}} > \overline{N}_{\mathrm{abs}} \end{cases} \tag{13b}$$

where $\gamma(s, x) \triangleq \int_0^x t^{s-1} e^{-t}\, dt$ denotes the lower incomplete gamma function, $\alpha_0^2 \triangleq \frac{\Gamma(1/\beta)}{\Gamma(3/\beta)}\sigma_{\mathrm{ISI}}^2$, and $\alpha_1^2 \triangleq \frac{\Gamma(1/\beta)}{\Gamma(3/\beta)}(\sigma_{\mathrm{u}}^2 + \sigma_{\mathrm{ISI}}^2)$. By substituting (13) in (10) we easily get the error probability as a function of the threshold.

B. Optimal Threshold

It is clear from (13) that the optimal threshold has to be lower than $\overline{N}_{\mathrm{abs}}$. By deriving the expression of P_{e} with respect N_{th} we obtain, for $(N_{\mathrm{th}} \le \overline{N}_{\mathrm{abs}})$:

$$\frac{dP_{\mathrm{e}}}{dN_{\mathrm{th}}} = p_0 \frac{dP_{\mathrm{e}}|_0}{dN_{\mathrm{th}}} + p_1 \frac{dP_{\mathrm{e}}|_1}{dN_{\mathrm{th}}} \tag{14}$$

where

$$\frac{dP_{\mathrm{e}}|_0}{dN_{\mathrm{th}}} = -\frac{\beta}{2\alpha_0\,\Gamma(1/\beta)} \exp\left[-\left(\frac{N_{\mathrm{th}} - \mu_{\mathrm{ISI}}}{\alpha_0}\right)^{\beta}\right] \tag{15a}$$

$$\frac{dP_{\mathrm{e}}|_1}{dN_{\mathrm{th}}} = \frac{\beta}{2\alpha_1\,\Gamma(1/\beta)} \exp\left[-\left(\frac{\mu_{\mathrm{u}} + \mu_{\mathrm{ISI}} - N_{\mathrm{th}}}{\alpha_1}\right)^{\beta}\right] \tag{15b}$$

By setting (14) to zero we obtain:

$$\frac{p_0}{\alpha_0} \exp\left[-\left(\frac{N_{\mathrm{th}} - \mu_{\mathrm{ISI}}}{\alpha_0}\right)^{\beta}\right] = \frac{p_1}{\alpha_1} \exp\left[-\left(\frac{\mu_{\mathrm{u}} + \mu_{\mathrm{ISI}} - N_{\mathrm{th}}}{\alpha_1}\right)^{\beta}\right]$$

that is

$$\ln\left(\frac{p_0}{\alpha_0}\right) - \left(\frac{N_{\mathrm{th}} - \mu_{\mathrm{ISI}}}{\alpha_0}\right)^{\beta} = \ln\left(\frac{p_1}{\alpha_1}\right) - \left(\frac{\mu_{\mathrm{u}} + \mu_{\mathrm{ISI}} - N_{\mathrm{th}}}{\alpha_1}\right)^{\beta}. \tag{16}$$

By denoting as N_{th}^* the solution of (16), the optimal threshold can be written as

$$N_{\mathrm{th}}^{(\mathrm{opt})} = \min\{N_{\mathrm{th}}^*, \overline{N}_{\mathrm{abs}}\}. \tag{17}$$

Thus, the error probability can be obtained through (10), by using (13), and (17), as well as the expressions of μ_{u}, μ_{ISI}, σ_{u}^2, and σ_{ISI}^2 derived in [12] for both the synchronous and the asynchronous case.

IV. Case Study

A. Optimal Threshold for ISI-Dominated Scenario

Consider the case $p_0 = \frac{\alpha_0}{\alpha_0 + \alpha_1}$, $p_1 = \frac{\alpha_1}{\alpha_0 + \alpha_1}$. The optimal threshold is derived by (16) with $\frac{p_0}{p_1} = \frac{\alpha_0}{\alpha_1}$, as follows

$$\frac{N_{\mathrm{th}} - \mu_{\mathrm{ISI}}}{\alpha_0} = \frac{\mu_{\mathrm{u}} + \mu_{\mathrm{ISI}} - N_{\mathrm{th}}}{\alpha_1} \Rightarrow N_{\mathrm{th}} = \frac{\alpha_0}{\alpha_0 + \alpha_1}\mu_{\mathrm{u}} + \mu_{\mathrm{ISI}}.$$

Thus the threshold minimizing the BEP is

$$N_{\rm th}^{*}=\frac{\sigma_{\rm ISI}}{\sigma_{\rm ISI}+\sqrt{\sigma_{\rm u}^2+\sigma_{\rm ISI}^2}}\mu_{\rm u}+\mu_{\rm ISI}. \tag{18}$$

By (10), (13), (17), and (18), we obtain

$$P_{\rm e}=\begin{cases}\frac{1}{2}-\frac{\gamma\left(\frac{1}{\beta},\left|\frac{\mu_{\rm u}}{\alpha_0+\alpha_1}\right|^{\beta}\right)}{2\Gamma\left(\frac{1}{\beta}\right)} & \text{for } N_{\rm th}^{*}<\overline{N}_{\rm abs}\\ p_{\rm fl}^{*} & \text{for } N_{\rm th}^{*}>\overline{N}_{\rm abs}\end{cases} \tag{19}$$

where, by defining $\overline{\alpha}_0\triangleq\alpha_0\ \mathrm{sgn}(\overline{N}_{\rm abs}-\mu_{\rm ISI})$, it is

$$p_{\rm fl}^{*}\triangleq\frac{1}{2}-\frac{\overline{\alpha}_0\gamma\left(\frac{1}{\beta},\left|\frac{\overline{N}_{\rm abs}-\mu_{\rm ISI}}{\alpha_0}\right|^{\beta}\right)+\alpha_1\gamma\left(\frac{1}{\beta},\left|\frac{\mu_{\rm u}+\mu_{\rm ISI}-\overline{N}_{\rm abs}}{\alpha_1}\right|^{\beta}\right)}{2(\alpha_0+\alpha_1)\Gamma\left(\frac{1}{\beta}\right)}.$$

Note that, in a ISI dominated scenario, $\sigma_{\rm u}^2\ll\sigma_{\rm ISI}^2$ and thus $p_0\to 1/2$, $p_1\to 1/2$. In other words, the proposed case coincides with the case of equiprobable symbols when the variance of the ISI dominates that of the useful signal. In such a case, from (17) and (18) we obtain:

$$N_{\rm th}^{(\rm opt)}\to\min\left\{\frac{\mu_{\rm u}}{2}+\mu_{\rm ISI},\overline{N}_{\rm abs}\right\}. \tag{20}$$

B. Maximum Transmitter Points Density Evaluation

In the general case, by setting the threshold to (20), it is

$$P_{\rm e}=\begin{cases}p(\mathrm{SIR},\mathrm{SINR}) & \text{for } \mu_{\rm u}/2+\mu_{\rm ISI}\le\overline{N}_{\rm abs}\\ p_{\rm fl}\left(\overline{N}_{\rm abs}\right) & \text{for } \mu_{\rm u}/2+\mu_{\rm ISI}>\overline{N}_{\rm abs}\end{cases} \tag{21}$$

where $\mathrm{SIR}\triangleq\mu_{\rm u}^2/\sigma_{\rm ISI}^2$, $\mathrm{SINR}\triangleq\mu_{\rm u}^2/(\sigma_{\rm u}^2+\sigma_{\rm ISI}^2)$, $p_{\rm fl}(\overline{N}_{\rm abs})$ is obtained from (10) by substituting $N_{\rm th}=\overline{N}_{\rm abs}$ in (13), and

$$p(\mathrm{SIR},\mathrm{SINR})\triangleq\frac{1}{2}-\frac{p_0\gamma\left[\frac{1}{\beta},(\rho\ \mathrm{SIR})^{\frac{\beta}{2}}\right]+p_1\gamma\left[\frac{1}{\beta},(\rho\ \mathrm{SINR})^{\frac{\beta}{2}}\right]}{2\Gamma\left(\frac{1}{\beta}\right)}$$

with $\rho\triangleq\Gamma(3/\beta)/4\Gamma(1/\beta)$. Now, we derive the maximum density of point transmitters before the saturation effect arises. To this aim, we substitute in (21) the expressions of $\mu_{\rm u}$, $\mu_{\rm ISI}$, SIR, and SINR as functions of $\lambda_{\rm a}$, derived in [12] for both the synchronous and the asynchronous case.

1) Synchronous Case: For Poisson concentration transmitters, the mean of useful and ISI components are

$$\mu_{\rm u}=N_{\rm tx}H_{\rm all}(T_{\rm b}) \tag{22a}$$

$$\mu_{\rm ISI}=\frac{N_{\rm tx}}{2}[H_{\rm all}(j+1)\,T_{\rm b}]-H_{\rm all}(T_{\rm b})] \tag{22b}$$

where $H_{\rm all}(t)$ is the so called collective impulse response resulting in $H_{\rm all}(t)=4\lambda_{\rm a}R\sqrt{\pi Dt}(2R+\sqrt{\pi Dt})$. The SIR and SINR result as in [12, eq. (84)].

2) Asynchronous Case: For timing asynchronous transmitters with uniformly distributed emissions in an activity interval $T_{\rm a}$, the mean of useful and ISI components result in

$$\mu_{\rm u}=8\lambda_{\rm a}R^2\sqrt{\pi D}\ \frac{N_{\rm tx}}{T_{\rm a}}\ \psi\left(T_{\rm b},T_{\rm a},\frac{\sqrt{\pi D}}{R}\right) \tag{23a}$$

$$\mu_{\rm ISI}=\frac{N_{\rm tx}}{2T_{\rm a}}\left(h_{j+1}-h_1\right) \tag{23b}$$

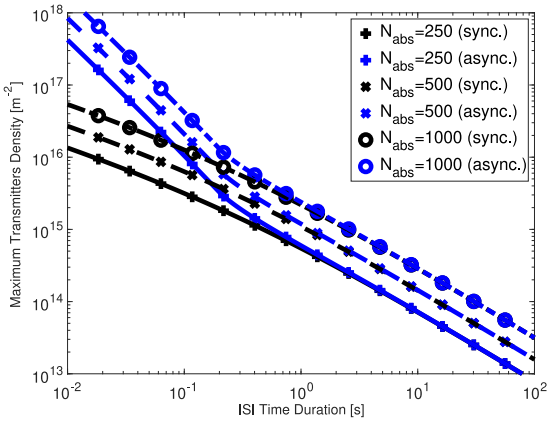

Fig. 2. Maximum transmitters density as a function of the ISI time duration.

where $h_k=8\lambda_{\rm a}R^2\sqrt{\pi D}\ \psi(kT_{\rm b},T_{\rm a},\frac{\sqrt{\pi D}}{R})$ and

$$\psi(t,T,x)\triangleq\begin{cases}\frac{2\sqrt{t^3}}{3}+\frac{t^2x}{4}, & \text{for } t\le T\\ \phi(t,T,x)+\frac{Tx}{2}\left(t-\frac{T}{2}\right) & \text{for } t>T\end{cases}$$

with $\phi(t,T,x)\triangleq\frac{2}{3}(\sqrt{t^3}-t\sqrt{t-T}+T\sqrt{t-T})$.

The SIR and SINR are obtained as in [12, eq. (85)]. By substituting (22) and (23), after some algebra (21) becomes

$$P_{\rm e}=\begin{cases}p(\mathrm{SIR},\mathrm{SINR}) & \text{for } \lambda\le\lambda_{\rm M}\\ P_{\rm e}\left(\overline{N}_{\rm abs}\right) & \text{for } \lambda>\lambda_{\rm M}\end{cases} \tag{24}$$

where $\lambda_{\rm M}$ represents the maximum transmitters density, that, for Poisson concentration (synchronous) transmitters, is

$$\lambda_{\rm M}=\frac{\overline{N}_{\rm abs}}{2N_{\rm tx}R\sqrt{\pi D(j+1)\,T_{\rm b}}\left(2R+\sqrt{\pi D(j+1)\,T_{\rm b}}\right)} \tag{25}$$

and, for timing (asynchronous) transmitters with uniformly distributed emissions in an activity interval $T_{\rm a}$, is

$$\lambda_{\rm M}=\frac{\overline{N}_{\rm abs}}{4R^2\sqrt{\pi D}\ \frac{N_{\rm tx}}{T_{\rm a}}\ \psi\left((j+1)\,T_{\rm b},T_{\rm a},\frac{\sqrt{\pi D}}{R}\right)}. \tag{26}$$

Note that, since SIR and SINR are increasing functions of the point transmitters density $\lambda_{\rm a}$, $\lambda_{\rm M}$ implies a floor value for the BEP. We also remark that, in both cases (synchronous and asynchronous), the maximum transmitters density $\lambda_{\rm M}$ linearly increases with the saturation level $\overline{N}_{\rm abs}$ and decreases with the number of emitted molecules $N_{\rm tx}$, the diffusion coefficient D, and the square of the receiver radius R. However, since the maximum number of absorbed molecules depends on the number of receptors over the cell surface, it is reasonable to assume $\overline{N}_{\rm abs}$ proportional to R^2 (the number of receptors increases as the area increases). Hence, $\lambda_{\rm M}$ should not substantially depend on the dimension of the receiver. It is clear that the dominant term at the denominator of (25) and (26) depends on the number j of the previously transmitted symbols which generate ISI. In Fig. 2 the maximum value of the transmitters density $\lambda_{\rm M}$ before the saturation effect arises is plotted as a function of the total ISI duration $(j+1)\,T_{\rm b}$, for both synchronous (25) and asynchronous (26) case, for different values of the saturation level $\overline{N}_{\rm abs}$. Due to the lower

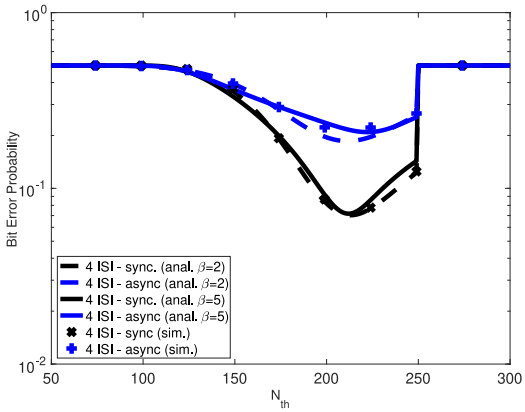

Fig. 3. BEP as a function of the threshold $N_{\rm th}$, with 4 ISI symbols and $\overline{N}_{\rm abs} = 250$. Comparison between analytical and simulation results.

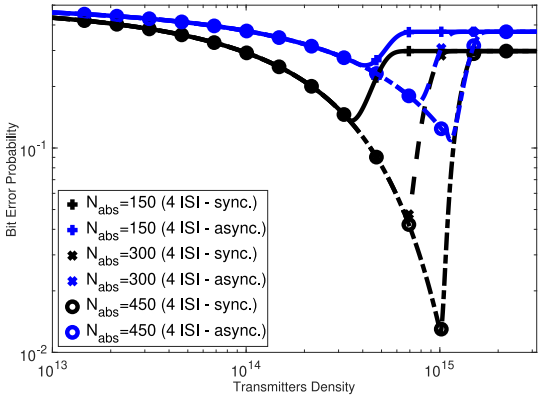

Fig. 4. BEP as a function of the point transmitters density $\lambda_{\rm a}$ with 4 ISI symbols, optimal threshold, and $\beta = 3.5$.

efficiency of the asynchronous transmission (less molecules hit the receiver with respect to the synchronous case), the receiver saturation effect arises for higher values of point transmitters density (compared to the case of synchronous transmission).

Such a result establishes that, in the considered scenario, differently from the case in [12] related to the fully absorbing receiver, ISI cannot be counteracted by indefinitely increasing the density of point transmitters.

C. Analytical and Simulation Results

In this section, we show the impact of the saturation effect on the BEP and we validate the analytical expression (13) through Monte Carlo simulations. To this aim, we assume the validity of (4) (that has already been verified in [3] by particle-based simulations) and, we compute $\mathsf{n}_{\rm rx}$ according to (6) by using the superposition of effects (note that, according to (8), each contribution contains both useful and ISI terms). Then $\overline{N}_{\rm abs}$ is considered according to (9) (saturation effect), compared to the threshold $N_{\rm th}$ and used (instead of $\mathsf{n}_{\rm rx}$) to count the error events. The resulting values for the bit error rate are finally averaged over 10^4 instantiations of the considered PPs. A receiver with radius $R = 5\mu$m, a bounded space of radius $R_{\rm a} = 50\mu$m, a diffusion coefficient $D = 120\mu\,\mathrm{m}^2\,/\,\mathrm{s}$, a bit time duration $T_{\rm b} = 0.2$s, an average number of emitted molecules per bit $N_{\rm tx} = 80$, and 4 ISI symbols are considered, according to [18], [19]. For what concerns the generalized Gaussian parameter, $\beta \in [2, 5]$ is considered [17].

In Fig. 3 the BEP is depicted as a function of the threshold $N_{\rm th}$ for a point transmitters density $\lambda_{\rm a} = 10^{15}\ \mathrm{m}^{-3}$, according to (10) and (13). As expected, the BEP drops to 1/2 as soon as the threshold $N_{\rm th}$ overcomes $\overline{N}_{\rm abs}$. Both Gaussian ($\beta = 2$) and generalized Gaussian ($\beta = 5$) approximations are considered for the analysis and compared to Monte Carlo simulations results. The figure shows a good agreement for both the synchronous and the asynchronous case. More precisely, $\beta = 2$ well fits the synchronous case, while $\beta = 5$ is the best fitting for the asynchronous case.

In Fig. 4 the BEP is shown as a function of the point transmitters density $\lambda_{\rm a}$ for the case of optimal threshold with different values of the saturation level $\overline{N}_{\rm abs}$. Here, an intermediate value $\beta = 3.5$ is chosen for both the synchronous and the asynchronous case. It can be observed that, as expected, asynchronous transmission implies higher values of $P_{\rm e}$ before the saturation effect arises.

V. Conclusion

A spatially distributed large-scale MCvD system is considered with a swarm of point transmitters and a not fully absorbing spherical receiver. An analytical model for the BEP in case of OOK modulation is obtained based on point processes theory for both synchronous and asynchronous transmitters. We show that, differently from the fully absorbing receiver case, if the density of the point transmitters increases over a given threshold, the BEP drops to a value close to 1/2 as a result of the saturation effect at the receiver side. The optimal values for point transmitters density are analytically determined and validated through Monte Carlo simulations.

References

[1] S. A. Salehi, H. Jiang, M. D. Riedel, and K. K. Parhi, "Molecular sensing and computing systems," *IEEE Trans. Mol. Biol. Multi-Scale Commun.*, vol. 1, no. 3, pp. 249–264, Sep. 2015.

[2] N.-R. Kim and C.-B. Chae, "Novel modulation techniques using isomers as messenger molecules for nano communication networks via diffusion," *IEEE J. Sel. Areas Commun.*, vol. 31, no. 12, pp. 847–856, Dec. 2013.

[3] H. B. Yilmaz, A. C. Heren, T. Tugcu, and C.-B. Chae, "Three-dimensional channel characteristics for molecular communications with an absorbing receiver," *IEEE Commun. Lett.*, vol. 18, no. 6, pp. 929–932, Jun. 2014.

[4] N. Farsad, H. B. Yilmaz, A. Eckford, C.-B. Chae, and W. Guo, "A comprehensive survey of recent advancements in molecular communication," *IEEE Commun. Surveys Tuts.*, vol. 18, no. 3, pp. 1887–1919, 3rd Quart., 2016.

[5] M. Pierobon and I. F. Akyildiz, "Diffusion-based noise analysis for molecular communication in nanonetworks," *IEEE Trans. Signal Process.*, vol. 59, no. 6, pp. 2532–2547, Jun. 2011.

[6] M. Pierobon and I. F. Akyildiz, "Capacity of a diffusion-based molecular communication system with channel memory and molecular noise," *IEEE Trans. Inf. Theory*, vol. 59, no. 2, pp. 942–954, Feb. 2013.

[7] M. Pierobon and I. F. Akyildiz, "A statistical–physical model of interference in diffusion-based molecular nanonetworks," *IEEE Trans. Commun.*, vol. 62, no. 6, pp. 2085–2095, Jun. 2014.

[8] T. Nakano, "Molecular communication: A 10 year retrospective," *IEEE Trans. Mol. Biol. Multi-Scale Commun.*, vol. 3, no. 2, pp. 71–78, Jun. 2017.

[9] Y. Deng, A. Noel, W. Guo, A. Nallanathan, and M. Elkashlan, "Analyzing large-scale multiuser molecular communication via 3-D stochastic geometry," *IEEE Trans. Mol. Biol. Multi-Scale Commun.*, vol. 3, no. 2, pp. 118–133, Jun. 2017.
[10] F. Zabini, "Spatially distributed molecular communications: An asynchronous stochastic model," *IEEE Commun. Lett.*, vol. 22, no. 7, pp. 1326–1329, Jul. 2018.
[11] F. Zabini, G. Pasolini, C. De Castro, and O. Andrisano, "On molecular communications via diffusion with multiple transmitters and multiple receivers," in *Proc. IEEE Global Commun. Conf. (GLOBECOM)*, 2018, pp. 206–212.
[12] F. Zabini, "Spatially distributed molecular communications via diffusion: Second-order analysis," *IEEE Trans. Mol. Biol. Multi-Scale Commun.*, vol. 5, no. 2, pp. 112–138, Nov. 2019.
[13] B. C. Akdeniz, N. A. Turgut, H. B. Yilmaz, C.-B. Chae, T. Tugcu, and A. E. Pusane, "Molecular signal modeling of a partially counting absorbing spherical receiver," *IEEE Trans. Commun.*, vol. 66, no. 12, pp. 6237–6246, Dec. 2018.
[14] E. Dinc and O. B. Akan, "Theoretical limits on multiuser molecular communication in Internet of nano-bio things," *IEEE Trans. NanoBiosci.*, vol. 16, no. 4, pp. 266–270, Jun. 2017.
[15] L. Felicetti, M. Femminella, and G. Reali, "Congestion control in molecular cyber-physical systems," *IEEE Access*, vol. 5, pp. 10000–10011, 2017.
[16] D. T. Gillespie, "The chemical Langevin equation," *J. Chem. Phys.*, vol. 113, no. 1, pp. 297–306, 2000.
[17] B.-H. Koo, C. Lee, H. B. Yilmaz, N. Farsad, A. Eckford, and C.-B. Chae, "Molecular MIMO: From theory to prototype," *IEEE J. Sel. Areas Commun.*, vol. 34, no. 3, pp. 600–614, Mar. 2016.
[18] G. Genc, Y. E. Kara, H. B. Yilmaz, and T. Tugcu, "ISI-aware modeling and achievable rate analysis of the diffusion channel," *IEEE Commun. Lett.*, vol. 20, no. 9, pp. 1729–1732, Sep. 2016.
[19] Y. Lu, X. Wang, M. D. Higgins, A. Noel, N. Neophytou, and M. S. Leeson, "Energy requirements of error correction codes in diffusion-based molecular communication systems," *Nano Commun. Netw.*, vol. 11, pp. 24–35, Mar. 2017.

Flavio Zabini (Member, IEEE) received the Laurea degree *(summa cum laude)* in telecommunications engineering and the Ph.D. degree in electronic engineering and computer science from the University of Bologna, Italy, in 2004 and 2010, respectively. In 2004, he developed his master's thesis with the University of California at San Diego, La Jolla. He was a visiting student with DoCoMo Eurolabs, Munich, Germany, in 2008, and a Postdoctoral Fellow with the German Aerospace Center, Cologne, Germany, from 2013 to 2014. He was with the IEIIT, CNR. He is currently a Researcher with the University of Bologna. His current research interests include random sampling techniques applied to sensor networks, performance-fairness tradeoff in communication systems, and molecular communications. He serves as an Associate Editor for the IEEE COMMUNICATION LETTERS and the *KSII Transactions on Internet and Information Systems*.

Barbara Maví Masini (Senior Member, IEEE) received the Laurea degree *(summa cum laude)* in telecommunications engineering and the Ph.D. degree in electronic, computer science, and telecommunication engineering from the University of Bologna, Italy, in 2001 and 2005, respectively. She is currently a Senior Researcher with the Institute for Electronics and for Information and Telecommunications Engineering, National Research Council (CNR) and an Adjunct Professor with the University of Bologna. She works in the area of wireless communication systems and her research interests are mainly focused on connected vehicles, from physical and MAC levels aspects up to applications and field trial implementations. Research is also focused on relay assisted communications, energy harvesting, and visible light communication. She is the Editor of IEEE ACCESS and *Computer Communication* (Elsevier). She is responsible for a number of National and International Projects on Vehicular Communications and Urban Intelligence.

Open Access funding provided by 'Alma Mater Studiorum - Università di Bologna' within the CRUI CARE Agreement